

# Relation Between First Arrival Time and Permeability in Self-Affine Fractures with Areas in Contact

LAURENT TALON<sup>1</sup>, HAROLD AURADOU<sup>1</sup> and ALEX HANSEN<sup>2,1</sup>

<sup>1</sup> *Univ. Pierre et Marie Curie-Paris6, Univ. Paris-Sud, CNRS, Lab. FAST, Bât. 502, Campus Univ., Orsay, F-91405, France.*

<sup>2</sup> *Department of Physics, Norwegian University of Science and Technology, N-7491 Trondheim, Norway*

PACS 83.80.Hj – Suspensions, dispersions, pastes, slurries, colloids

PACS 46.50.+a – Fracture mechanics, fatigue and cracks

PACS 62.20.mt – Cracks

**Abstract** – We demonstrate that the first arrival time in dispersive processes in self-affine fractures are governed by the same length scale characterizing the fractures as that which controls their permeability. In one-dimensional channel flow this length scale is the aperture of the bottle neck, i.e., the region having the smallest aperture. In two dimensions, the concept of a bottle neck is generalized to that of a minimal path normal to the flow. The length scale is then the average aperture along this path. There is a linear relationship between the first arrival time and this length scale, even when there is strong overlap between the fracture surfaces creating areas with zero permeability. We express the first arrival time directly in terms of the permeability.

Due to their role in the flow properties of tight and low permeability reservoirs such as shale gas reservoirs and carbonate reservoirs, and on contaminant transport e.g. in connection with waste storage, the study of transport in fractures is still a very vigorous field [1–4]. Most present theoretical efforts attempts to relate the transport properties of fractures to the statistics of the aperture fields through analytical models based on statistical averages, weak disorder perturbation expansions [5], mean-field approximations or simplified aperture models [6]. We also mention the work of Zhan and Yortsos [7] where a method to deduce the heterogeneities of a permeability distribution from the concentration arrival time field was proposed.

Due to the surface roughness, i.e., the heterogeneities of the aperture field, these relations provide satisfactory results only over a finite range of conditions and do not permit to predict the behavior of a fracture with large heterogeneities in aperture field. One of the main difficulties is to correctly take into account the increasing influence of the contact area as the fracture aperture is decreased [8–11]. We analyze in this Letter the dispersion problem at finite Péclet number and identify the proper aperture measure for this problem, taking into account severe heterogeneities such as large contact zones. Our main focus is on the breakthrough time, i.e., the time at which the tracer appears at a given position. The

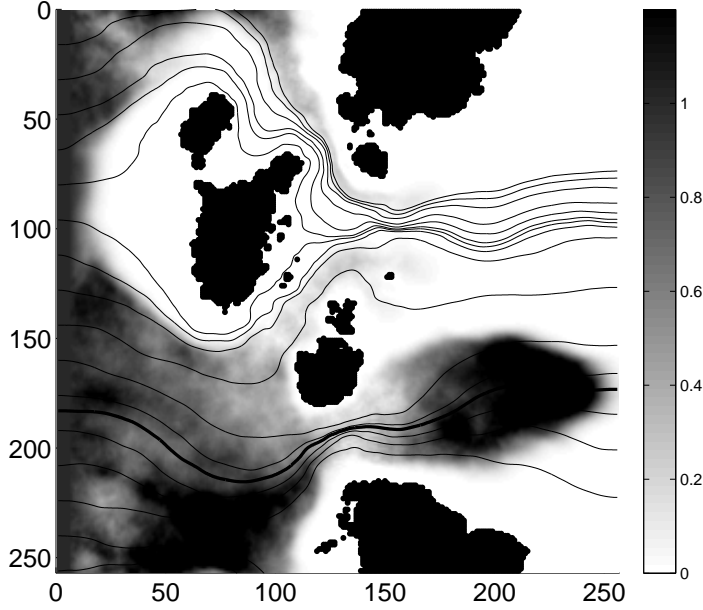


Fig. 1: Fluid flows in a self-affine aperture field seen from above. The curves are the streamlines of the flow field. The streamlines have been found using the Kirchhoff method. We have then used the Lattice Boltzmann method to simulate dispersion fixing the Péclet number at 10. The tracer concentration is shown on a grey scale where darker means higher concentration. Areas where the aperture is zero — i.e., the fracture surfaces are in contact — are shown as black.

surprising result that we find is that this aperture is the same as the one controlling the permeability [12, 13].

There are now numerous experimental studies and field observations that demonstrate that natural fractures have a self-affine roughness [14–18] — for a review, see Bonamy and Bouchaud [19]. Self-affine fractures are characterized by a scaling invariance of the statistical properties of the surface roughness under a rescaling of the distances by a factor  $\lambda$  in the average fracture plane and a rescaling  $\lambda^\zeta$  of the heights. Here  $\zeta$  is the Hurst or roughness exponent which takes value close to 0.8 for rocks such as granite [20] and values close to 0.5 for porous rocks like sandstone [21, 22].

We consider in this work synthetic self-affine fracture surfaces that have been generated using a Fourier method [23, 24]. The fracture is modeled by matching the fracture surface with an opposite flat surface. Since we use the Reynolds approximation, this correctly models flow in fractures as it is only the aperture that enters the flow equations. We define the fracture aperture  $H(\vec{r})$  as the distance between the two surfaces at position  $\vec{r}$ . In the present work, the rough surface progressively approaches the flat surface one and the aperture of overlapping regions is set to zero. Hence,  $H(\vec{r}) > 0$  where there is no overlap and  $H(\vec{r}) = 0$  where there is overlap.

The flow field is determined for a fixed pressure difference between the fracture inlet and outlet by solving the finite differenced Reynolds equations through LU decomposition. The total volume entering the fracture per width and time at the inlet is proportional to the pressure  $\Delta P$  over the fracture, and is given by

$$Q = -\frac{K}{L\mu}\Delta P, \quad (1)$$

where  $K$  is the permeability and  $\mu$  the viscosity of the fluid.  $L$  is the length of the fracture.

The breakthrough time is typically obtained by summing along each streamline the

local time of convection [25–27]. This method does, however, not take into account diffusion between and along the streamlines. We have instead discretized the velocity field on a square lattice with nearest-neighbor and next nearest-neighbor connections. If we assume that the dispersion time between neighboring nodes is the inverse of the velocity component along the vector between them, we have then introduced diffusion into the dispersion process. This is so since a given tracer particle will not follow the streamlines but move between the nodes via projected velocity vectors. We add to this description the analysis of Stern [28] of the first arrival time of a diffusive process with or against a convective velocity field, making it possible to tune the Péclet number. In order to find the first arrival time, we use the optimal path algorithm of Hansen and Kertesz [29]. We have verified our algorithm by comparing it to a two-dimensional Lattice Boltzmann method [30]. Fig. 1 shows the tracer concentration in gray levels at breakthrough with Péclet number  $Pe = 10$  based on the Lattice Boltzmann method. In the following, we do not discuss any dependence of our results on the Péclet number. The numerical experiments we report have been done at  $Pe = 10$  as a reasonable value. Other values add nothing significant.

Transport properties of fractures are often characterized by equivalent or apparent apertures — such as the hydraulic, mass balance or electrical apertures — which refers to the aperture of a fracture with flat and parallel walls having the same property as the original fracture. In practice, equivalent apertures are estimated from hydraulic and conservative tracer tests. The mass balance aperture  $b_m$  is defined as the ratio between the fluid flux  $Q$  and the averaged fluid velocity  $\bar{u}$  [31,32]. In practice, the average fluid velocity  $\bar{u}$  equals the average of the velocities of all fluid particles and should be derived from the average residence time determined from the moments of the time distribution of the measured tracer breakthrough curve [31]. Here we connect the first arrival time,  $\tau_{min}$ , to the average fluid velocity  $\bar{u}$  by the expression  $\bar{u} = L/\tau_{min}$ , as proposed by Guimerà and Carrera [32]. Since the pressure gradient is kept fixed, the mass balance aperture  $b_m = Q/\bar{u}$  is proportional to  $K\tau_{min}$ .

Before considering two-dimensional fractures, i.e., fractures where the aperture is orthogonal to a two-dimensional fracture plane, we consider a *one-dimensional* version of the problem, i.e., a fracture where the aperture is orthogonal to a fracture line. We introduce a cartesian coordinate system with the  $x$  axis along the line which now constitutes the flat surface. Let us set  $a = \min_x H(x)$ . We then define

$$h(x) = H(x) - a . \quad (2)$$

When  $a \leq 0$ , the fracture is closed and hence the permeability is zero. For positive  $a$ , it is this parameter that controls the permeability of the fracture in the lubrication approximation [13]. The permeability is in this limit given by the expression

$$\frac{L}{K} = \int_0^L \frac{d\xi}{k(c\xi + a)^3} , \quad (3)$$

where  $k$  and  $c$  are two parameters.  $c$ , the topothesis which characterizes the roughness of the aperture field, is a length scale, and  $k$  has the units of permeability. For large  $a$ , this gives rise to the scaling relation

$$K \sim La^3 , \quad (4)$$

whereas for intermediate  $a$ , we find

$$K \sim La^{3-1/\zeta} . \quad (5)$$

For small  $a$ , the permeability is completely controlled by the region where  $h(x) = 0$ , and the continuum approach behind eq. (3) breaks down. We then find that the permeability is given by

$$K \sim L^0 a^3 . \quad (6)$$

We now calculate  $\tau_{\min}$  using the lubrication approximation and in the infinite Péclet number limit where diffusion is absent. The first tracer to traverse the rough channel is the one which has traveled along the streamline located midway between the walls *i.e.* where the velocity is at its maximum. The time this has taken is  $\tau_{\min}$ , and it is given by

$$\tau_{\min} = \int_0^L \frac{dx}{u(x)}, \quad (7)$$

where  $u(x)$  is the maximal velocity at position  $x$  along the channel which is proportional to the flow rate over the local aperture in the lubrication approximation. We have thus

$$\tau_{\min} \propto \frac{1}{Q} \int_0^L (h(x) + a) dx. \quad (8)$$

Combining eqs.(1) and (8), we get

$$\tau_{\min} K = \frac{L\mu}{\Delta P} \int_0^L (h(x) + a) dx. \quad (9)$$

This integral may be performed by using order statistics [13]: We order the function  $h(x) \rightarrow h[\xi] = h(x[\xi])$  such that  $h[\xi_1] \leq h[\xi_2]$  when  $\xi_1 \leq \xi_2$ . For a self-affine profile we have that  $h[\xi] \sim \xi^\zeta$ , and eq. (8) becomes

$$\tau_{\min} K = \frac{L\mu}{\Delta P} \int_0^L (c\xi^\zeta + a) d\xi = \frac{\mu}{\Delta P} [cL^{2+\zeta} + aL^2], \quad (10)$$

where  $c$  is a constant. Hence, we have the central result for a one-dimensional channel

$$\tau_{\min} K = A + Ca, \quad (11)$$

where  $A \propto L^{2+\zeta}$  and  $C \propto L^2$ . Hence, we see that it is the minimum aperture  $a$  which controls the first arrival time  $\tau_{\min}$ . This is the same aperture that controls the permeability, see eqs. (4) – (6). This is a somewhat surprising result, since at the minimal aperture location, because of mass conservation, the flow rate is maximal. Consequently, the time in the bottle neck effect has a small contribution to the integral eq. (7). However, the bottle neck controls the total flow rate, and this, in turn, controls the first arrival time.

As described in Talon et al. [12, 13], the extrapolation of the bottle neck effect to a two-dimensional fracture is not straight forward since the minimal aperture point is easily bypassed by the flow. However, it is possible to generalize the concept to two dimensions by replacing the minimal aperture  $a$  by the *minimal path aperture*. In order to introduce this concept, we orient our fracture such that the one of the edges parallel to the average flow direction follows the  $x$  axis. The  $y$  axis follows the edge where the tracer is injected and the  $z$  axis is orthogonal to the average fracture plane. Hence,  $0 \leq x \leq L$  and  $0 \leq y \leq W$ . We define  $\mathcal{C}(x)$  as a path starting at  $(x, y = 0)$  and ending at  $(x', y = W)$  without crossing itself. Hence, we define the quantity

$$B(x) = \frac{1}{WL} \left[ \min_{\mathcal{C}(x)} \int_{\mathcal{C}(x)} d\vec{\ell} \cdot \vec{e}_y(\vec{\ell})^3 \right]^{1/3}. \quad (12)$$

This is the minimal average fracture opening over all paths starting at  $(x, 0)$  and ending anywhere along the opposite edge at  $y = W$ . This quantity corresponds to  $H(x)$  in the one-dimensional case. The *minimal path aperture* is defined as

$$b_c = \min_x B(x), \quad (13)$$

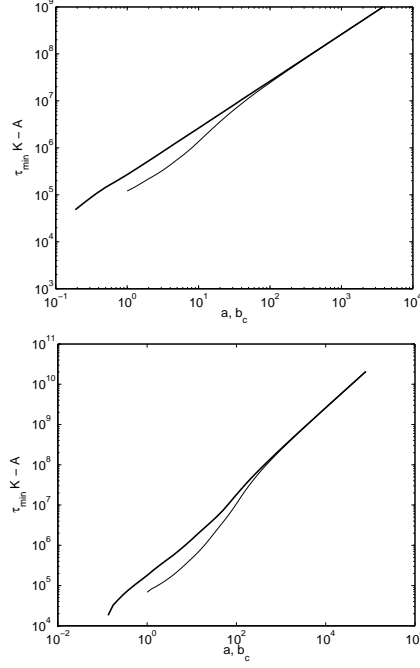


Fig. 2: Loglog plot of  $\tau_{\min}K - A$  as function of  $a$  and  $b_c$  for  $\zeta = 0.3$  (upper) and  $\zeta = 0.8$  (lower). The solid curves are for  $\tau_{\min}K - A$  vs.  $b_c$ , whereas the broken curve is for  $\tau_{\min}K - A$  vs.  $a$ . We determine  $A$  by varying it until we obtain the best possible power law. In both figures, the straight portions of the curves have unit slope as indicated in eq. (19). The curves are based on one sample of size  $512 \times 512$  for each roughness.

corresponding to the smallest aperture  $a$  in the one-dimensional case. We finally define

$$b(x) = B(x) - b_c, \quad (14)$$

in the same way we defined  $h(x)$  in eq. (2) in the one-dimensional case.

The central idea in Talon et al. [13] was that the two definitions  $b_c$  and  $b(x)$  could replace  $a$  and  $h(x)$  in the one-dimensional case in the permeability integral (3). After ordering  $b(x) \rightarrow b[\xi]$ , we find that  $b[\xi] \sim \xi^\beta$ , where  $\beta = 1.5$  for  $\zeta = 0.8$  and  $\beta = 1.2$  for  $\zeta = 0.3$ . The intermediate scaling regime (5) then is replaced by

$$K \sim WLb_c^{3-1/\beta}, \quad (15)$$

whereas the large and small scale regimes become respectively

$$K \sim WLb_c^3, \quad (16)$$

and

$$K \sim WL^0 b_c^3. \quad (17)$$

Numerical experiments based on solving the Kirchhoff equations give

$$K \sim \begin{cases} WLb_c^{2.25 \pm 0.02} & \text{for } \zeta = 0.8, \\ WLb_c^{2.16 \pm 0.02} & \text{for } \zeta = 0.3, \end{cases} \quad (18)$$

for the intermediate regime. The results are very close to the prediction of eq. (15).

By following exactly the same procedure for the first arrival time, i.e., replace  $h(x)$  by  $b(x)$  and  $a$  by  $b_c$  in eq. (8), we find

$$\tau_{\min}K = A + Cb_c, \quad (19)$$

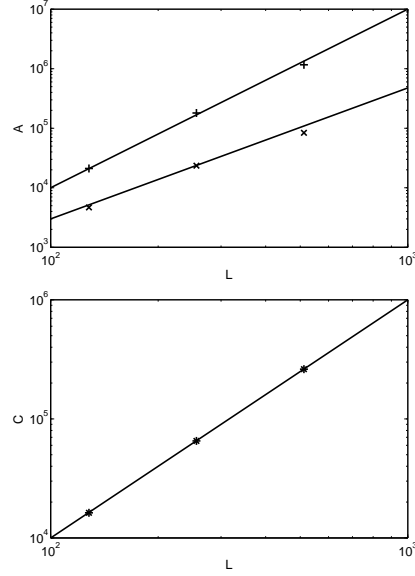


Fig. 3: Scaling of coefficients  $A$  (upper figure) and  $C$  (lower figure) defined in eq. (19). The straight lines are best fits and have slopes 3 for the  $\zeta = 0.8$  data (+) and 2.2 for the  $\zeta = 0.3$  data (x) in the upper figure. The theoretical values are 2.8 and 2.3 respectively. In the lower figure, the best fit has slope 2.0 for both the  $\zeta = 0.8$  and  $\zeta = 0.3$  data. The theoretical value is 2.

where  $A \propto WL^{2+\zeta}$  and  $C \propto WL^2$ . Fig. 3 shows  $A$  and  $C$  as a function of  $L$  verifying these two scaling laws. We show in fig. 2,  $\tau_{\min}K$  as a function of  $b_c$  and of  $a$ . We see that the linearity of  $\tau_{\min}K$  is verified for the entire range of  $b_c$  values, whereas it is only true for large values of  $a$ . This is where  $a$  and  $b_c$  begin to coincide.

Hence, we have verified that the minimal path aperture  $b_c$  controls *both* the permeability  $K$  and the minimal time  $\tau_{\min}$ . This, together with eq. (19) constitute two main results of this Letter.

Since the first arrival time and the permeability are controlled by the same aperture, it is possible to eliminate the aperture between them. Hence, we may express the first arrival time directly in terms of the permeability by combining eqs. (16) – (19). We show in Fig. 4  $\tau_{\min}$  vs.  $K$  for two roughnesses,  $\zeta = 0.8$  and  $\zeta = 0.3$ . We expect that for small  $K$ ,  $\tau_{\min} \sim A/K^1$ , where  $A$  is defined in eq. (19). For large  $K$ , we expect  $\tau_{\min} \sim C/K^{2/3}$ . For intermediate  $K$ , we expect  $\tau_{\min} \sim A/K + C/K^{0.56}$  when  $\zeta = 0.8$  and  $\tau_{\min} \sim A/K + C/K^{0.54}$  for  $\zeta = 0.3$ .  $C$  is defined in eq. (19). Straight lines with the appropriate slopes have been added in Fig. 4. For the intermediate region, we have used only the term proportional to  $C$ .

We have in this Letter shown that the permeability and the first arrival time in dispersive processes are controlled by the same aperture length scale in self-affine fractures. We have also shown that the functional relation between the first arrival time and this aperture is linear, see eq. (19). The appropriate aperture is the minimal path aperture defined in eqs. (14) and (13). It is a generalization of the concept of the narrowest constriction that controls both the permeability and the first arrival time in one-dimensional fracture systems. Whereas the scaling properties we report are specific to self-affine aperture fields, the method of analysis based on optimal paths is not.

\*\*\*

We thank J. P. Hulin for many interesting discussions. A. H. thanks the Université de Paris-Sud 11 for financial support. H. A. and L. T. thanks the PICS “The Physics

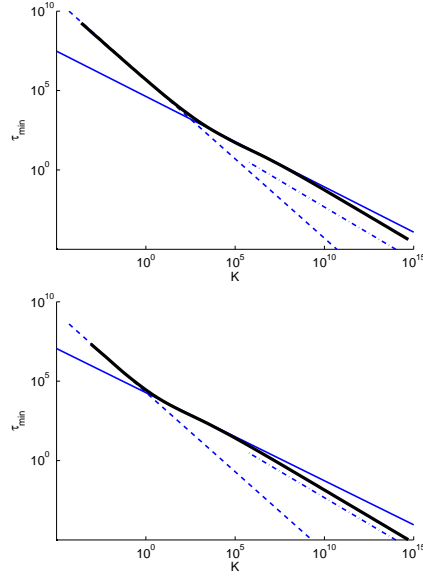


Fig. 4: First arrival time  $\tau_{\min}$  vs. permeability  $K$  for  $\zeta = 0.8$  (upper figure) and  $\zeta = 0.3$  (lower figure). Each curve is based on one sample of size  $512 \times 512$ . The slopes of the straight lines are given in the main text.

of Geological Complex System” and the Réseaux de Thématiques de Recherches Avancées “Triangle de la Physique” for financial support.

## REFERENCES

- [1] H. ABELIN and L. BIRGERSSON and L. MORENO and H. WIDEN and T. AGREN and I. NERETNIEKS, *Water Resour. Res.*, **27** (1991) 3119
- [2] National Research Council, Committee on Fracture Characterization and Fluid Flow *Rock Fractures and Fluid Flow: Contemporary Understanding and Applications* (National Academy Press, Washington DC) 1996
- [3] S. A. HOLDITCH, *J. Petr. Tech.*, **58** (2006) 86
- [4] J. Y. WANG and S. A. HOLDITCH and D. A. MCVAY, *SPE, Hydraulic Fracturing Technology Conference held in Woodlands, Texas, Jan. 19–21 2009*
- [5] A. A. KELLER and P. V. ROBERTS and P. K. KITANIDIS, *Geophys. Res. Lett.*, **22** (1995) 1425
- [6] F. BAUGET and M. FOURAR, *J. Contam. Hydrol.*, **100** (2008) 137
- [7] L. ZHAN and Y. C. YORTSOS, *Phys. Rev. E*, **62** (2000) 863
- [8] K. MATSUKI and Y. CHIDA and K. SAKAGUCHI and P. W. J. GLOVER, *Int. J. Rock Mech. and Mining Sci.*, **43** (2006) 726
- [9] N. WATANABE and N. HIRANO and N. TSUCHIYA, *Water Resour. Res.*, **44** (2008) W06412
- [10] N. WATANABE and N. HIRANO and N. TSUCHIYA, *J. Geophys. Res.*, **114** (2009) B04208
- [11] K. NEMOTO and N. WATANABE and N. HIRANO and N. TSUCHIYA, *Earth and Planet. Sci. Lett.*, **281** (2009) 81
- [12] L. TALON and H. AURADOU and A. HANSEN, *Water Resour. Res.*, **46** (2010) W07601
- [13] L. TALON and H. AURADOU and A. HANSEN, *Phys. Rev. E*, **82** (2010) 046108
- [14] W. L. POWER and T. E. TULLIS and S. R. BROWN and G. N. BOITNOTT and C. H. SCHOLZ, *Geophys. Res. Lett.*, **14** (1987) 29
- [15] E. BOUCHAUD and G. LAPASSET and J. PLANÈS, *Europhys. Lett.*, **13** (1990) 73
- [16] C. Y. POON and R. S. SAYLES and T. A. JONES, *J. Phys. D Appl. Phys.*, **25** (1992) 1269
- [17] K. J. MÅLØY and A. HANSEN and E. L. HINRICHSEN and S. ROUX, *Phys. Rev. Lett.*, **68** (1992) 213 (1992).
- [18] S. SCHMITTBUHL and S. GENTIER and S. ROUX, *Geophys. Res. Lett.*, **20** (1993) 639

- [19] D. BONAMY and E. BOUCHAUD, *Phys. Rep.*, **498** (2011) 1
- [20] D. AMITRANO and J. SCHMITTBUHL, *J. Geophys. Res. solid Earth*, **107** (2002) 2375
- [21] J. M. BOFFA and C. ALLAIN and J. P. HULIN, *Eur. Phys. J. Appl. Phys.*, **2** (1998) 281
- [22] L. PONSON and H. AURADOU and P. VI/’E and J. P. HULIN, *Phys. Rev. Lett.*, **97** (2006) 125501
- [23] D. Turcotte *Fractals and Chaos in Geology and Geophysics* (Cambridge University Press, Cambridge) 1997
- [24] M. SAHIMI, *Phys. Rep.*, **306** (1998) 213
- [25] L. MORENO and Y. W. TSANG and C. F. TSANG and F. V. HALE and I. NERETNIE, *Water Resour. Res.*, **24** (1988) 2033
- [26] A. A. KELLER and P. V. ROBERTS and M. J. BLUNT, *Water Resour. Res.*, **35** (1999) 55
- [27] R. METTIER and G. KOSAKOWSKI and O. KOLDITZ, *Ground Water*, **44** (2006) 687
- [28] F. STERN, *Mathem. Magaz.*, **48** (1975) 200
- [29] A. HANSEN AND J. KERTESZ, *Phys. Rev. Lett.*, **93** (2004) 040601
- [30] L. TALON and J. MARTIN and N. RAKOTOMALALA and D. SALIN and Y. C. YORTSOS, *Water Resour. Res.*, **39** (2003) 1135
- [31] NameY. W. Tsang *Water Resour. Res.*, **28** (1992) 1451
- [32] J. GUIMERÀ and J. CARRERA, *J. Contaminant Hydrol.*, **41** (2000) 261



